

CHAPTER 5

Results and Discussion (Part II):

ITO/Au/ITO Multilayer Films

Deposition and properties of the effects of an Au intermediate layer on ITO films are investigated in this chapter. The ITO/Au/ITO multilayer films were synthesized by using the ultrasonic spray pyrolysis technique for the ITO layer and the sputtering technique for the Au layer. Properties such as thickness, crystal structure, morphology, optical properties and electrical properties were measured and analyzed.

5.1 Film preparation

5.1.1 Starting solution preparation

The starting solution of the ITO layer was the solution of the ITO film doped with 5 at.% Sn. This condition was chosen for study in this part because this film showed the best conditions in the previous work (Chapter 4). The starting solution preparation was the same as in Chapter 4.

5.1.2 Film deposition

The ITO/Au/ITO multilayer films were prepared by 2 techniques. The ITO layers were deposited by the ultrasonic spray pyrolysis technique and the metallic layer of Au was coated between the ITO layers via the sputtering technique with thickness in the range of 0-20 nm. The schematic diagram of the ITO/Au/ITO multilayer films fabrication process is shown in Figure 5.1. The diagram can be divided into 3 steps. First, the starting solution was sprayed onto a microscope glass substrate heated at 350°C by using ultrasonic spray pyrolysis in air. The distance between the nozzle and the substrate was 20 cm with nozzle frequency of 34 kHz and spray rate 2.5 ml/min for 1.5 min. The samples after coating were subsequently annealed in an electric furnace at 500°C for 1 hour using a heating/cooling rate of

5°C/min. Then, the intermediate layer (Au) was coated on the ITO layer via a sputtering process in the range of 0-20 nm of thickness in vacuum. Finally, the top ITO layer was re-sprayed on the Au layer with the same conditions as the ITO lower layer and annealed again in at 500°C for 1 hour.

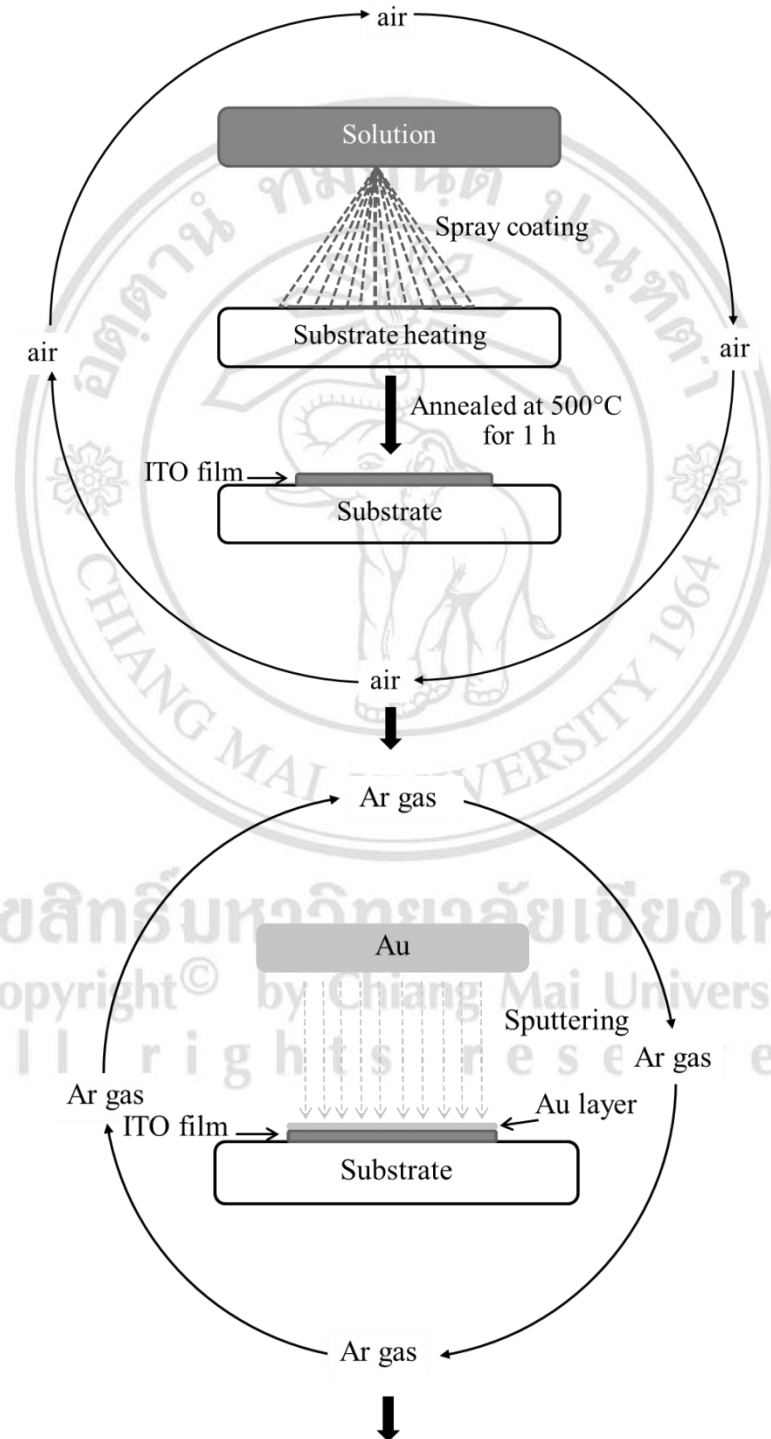


Figure 5.1 Schematic diagram of ITO/Au/ITO multilayer film preparation.

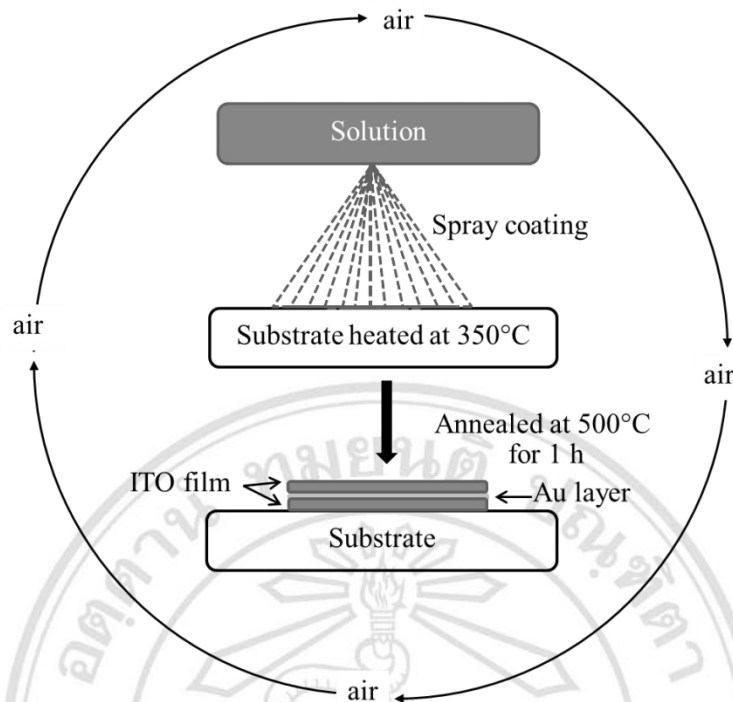


Figure 5.1 Schematic diagram of ITO/Au/ITO multilayer film preparation (continued).

5.2 Results and discussion

Images of the ITO/Au/ITO multilayer films with different Au intermediate layer thickness are shown in Figure 5.2. It was seen that the transparency of films decreased with increasing Au intermediate layer thickness and the color of samples changed to blue with added Au intermediate layer. The characterizations as thickness, crystal structure, morphology optical and electrical properties of these films are described in the following sections.

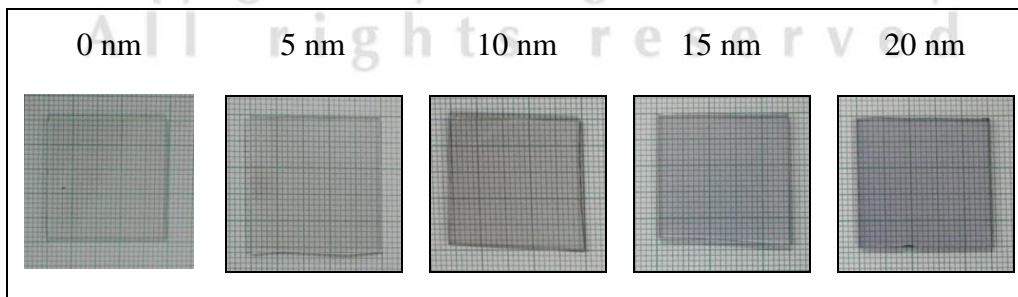


Figure 5.2 Images of the ITO/Au/ITO multilayers films with different Au intermediate layer thicknesses.

5.2.1 Thickness

Figure 5.3 shows the cross section microstructures of ITO/Au/ITO multilayer films with different Au intermediate layer thickness, which were investigated by SEM technique (Quanta 200 3D Dual Beam Focused Ion Beam). It was observed that the films grew well on the glass substrate. Film thicknesses were estimated from these SEM images and are listed in Table 5.1. All multilayer films showed similar thicknesses, which were in the range 200-300 nm

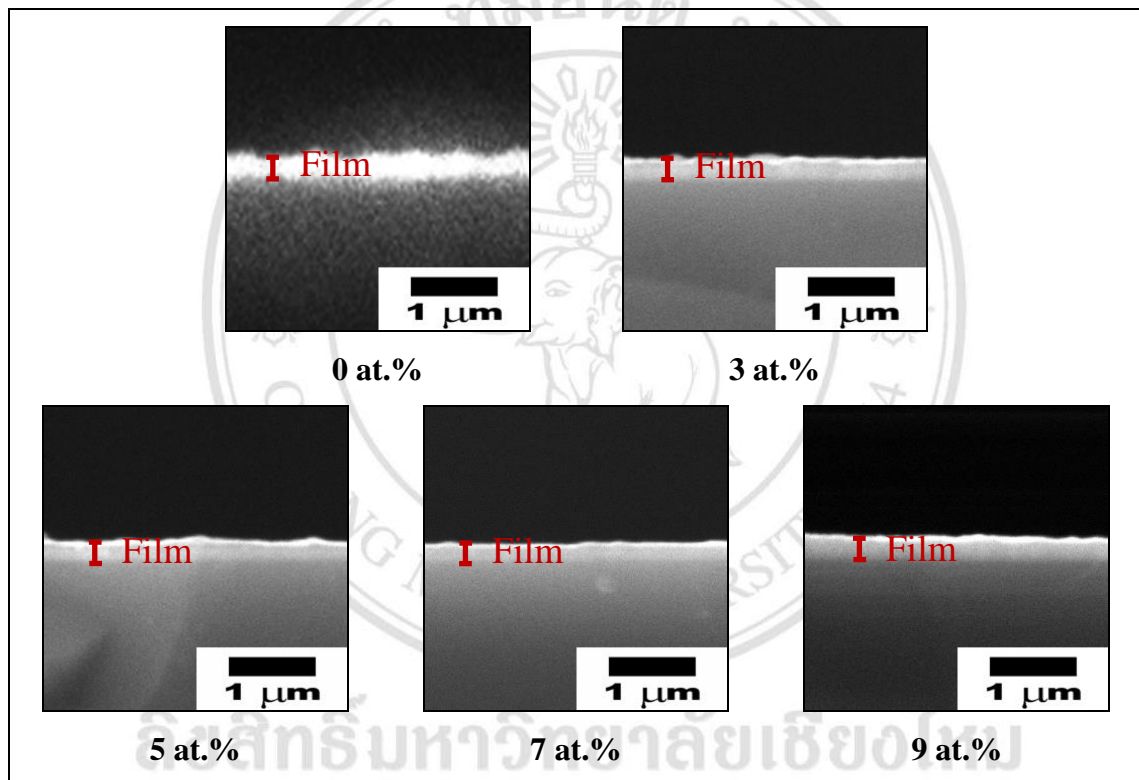


Figure 5.3 The cross section microstructures of ITO/Au/ITO multilayers films with different Au intermediate layer thicknesses.

Table 5.1 Thicknesses of ITO/Au/ITO multilayer films with different Au intermediate layer thicknesses.

Au intermediate layer thickness (nm)	Film thickness (nm)	
	Value	SD
0	242	29
5	228	28
10	255	27
15	207	18
20	264	17

5.2.2 Crystal structure

The XRD patterns of ITO/Au/ITO multilayer films with different Au intermediate layer thickness are presented in Figure 5.4. Both single layer (0 nm Au) and multilayer films were identified as the cubic structure of In_2O_3 . In addition, ITO multilayer films with 15-20 nm of Au layer were identified with small phase as (111) plane of Au metal. For the single layer film, the intensities of (222) and (400) planes were close and the intensity of the (222) plane increased with increasing Au interlayer thickness. The (400) plane increased with the Au layer at 5 nm but this plane decreased with Au layer more than 5 nm. The change of XRD spectra of multilayer films depended upon the Au interlayer thickness, which effectively promoted crystallization in the (222) plane of the top ITO layer [54]. It may be speculated that this plane of the top ITO layer has the same growth mode direction as the bottom Au (111) layer [8].

The crystallite sizes of multilayers films with different Au intermediate layers are listed in Table 5.2. The crystallite sizes of these films can be calculated from FWHM values of (222) and (400) peaks by equation 3.2 and the FWHM values were obtained from the XRD patterns. It was found that the crystallite sizes of the (222) peak of all films were similar and were

larger than the crystallite sizes of the (400) peak. Moreover, the trend of crystallite sizes of the (400) peak were opposite to the trend of the intensity of this peak.

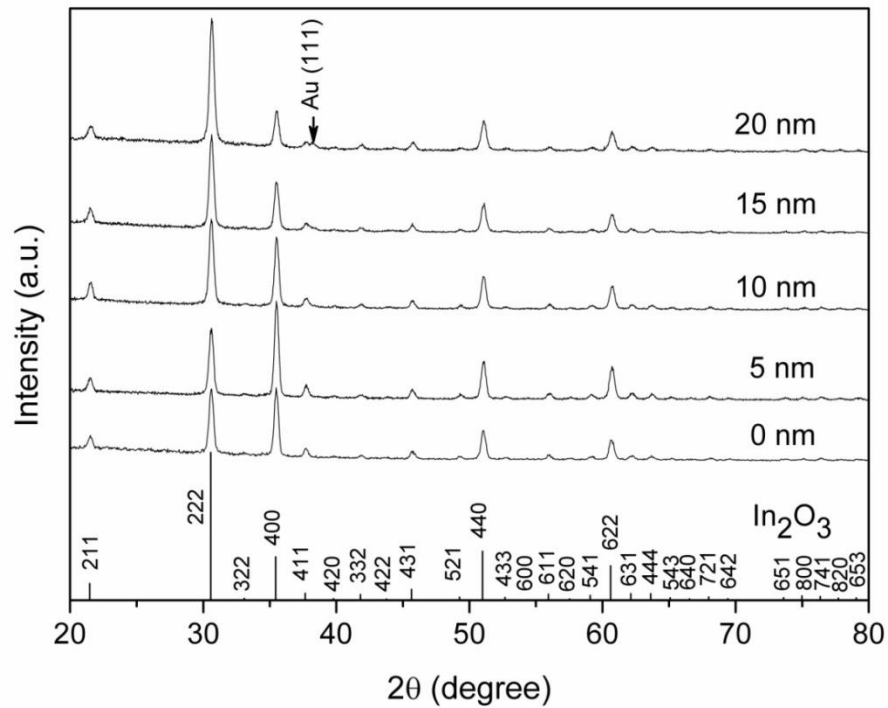


Figure 5.4 XRD patterns of ITO/Au/ITO multilayer films with different Au intermediate layer thicknesses.

Table 5.2 Crystallite size of (222) and (400) plane of ITO/Au/ITO multilayer films with different Au intermediate layer thicknesses.

Au intermediate layer thickness (nm)	Crystallite size (nm)	
	hkl (222)	hkl (400)
0	39.34	37.59
5	38.50	36.43
10	38.45	35.53
15	38.92	34.37
20	37.05	33.34

5.2.3 Morphology

Surface morphologies of ITO/Au/ITO multilayer film with different Au intermediate layer thickness were investigated by SEM and AFM technique and are shown in Figure 5.5 and 5.6.

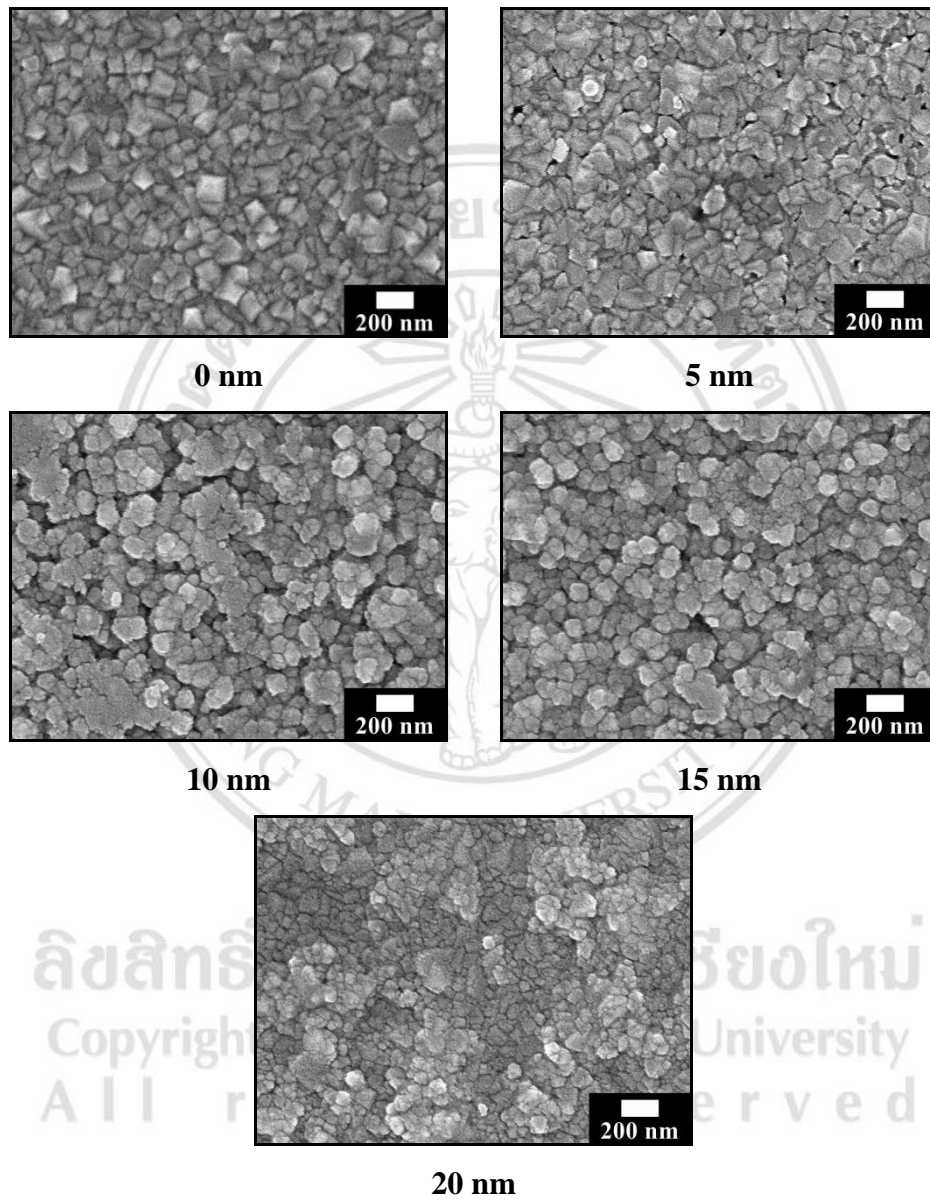


Figure 5.5 SEM images of ITO/Au/ITO multilayer films with different Au intermediate layer thicknesses.

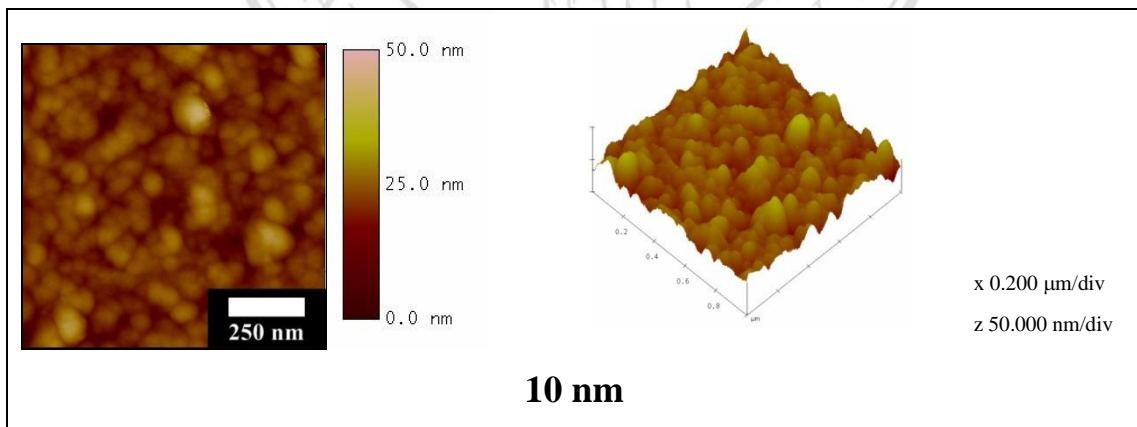
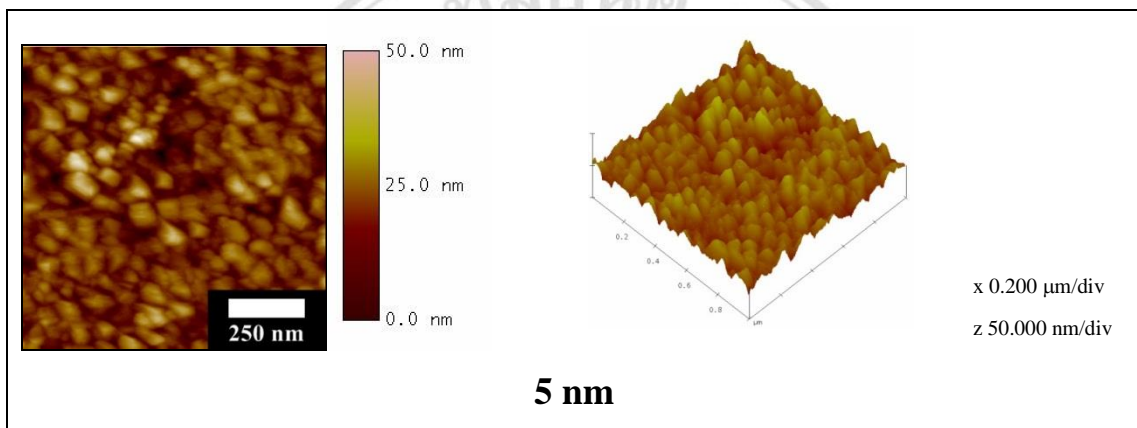
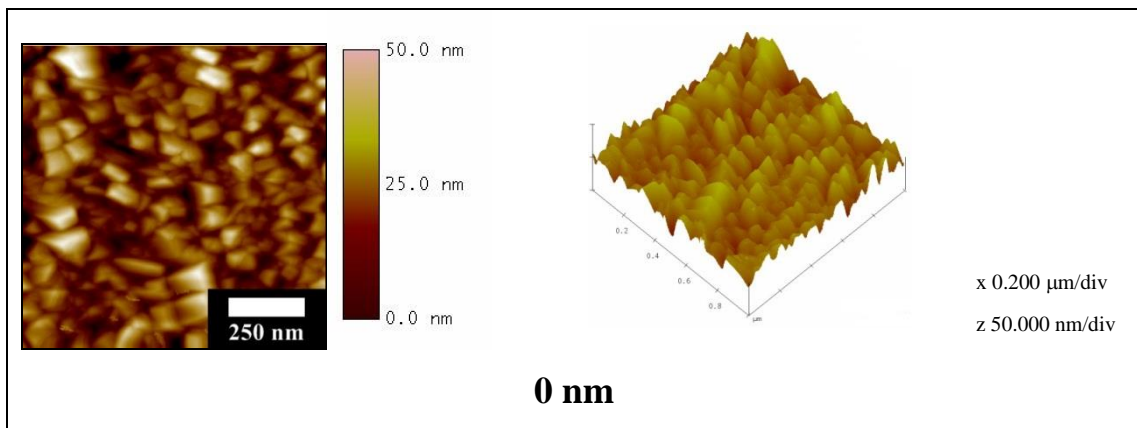


Figure 5.6 AFM images of ITO/Au/ITO multilayer films with different Au intermediate layer thicknesses.

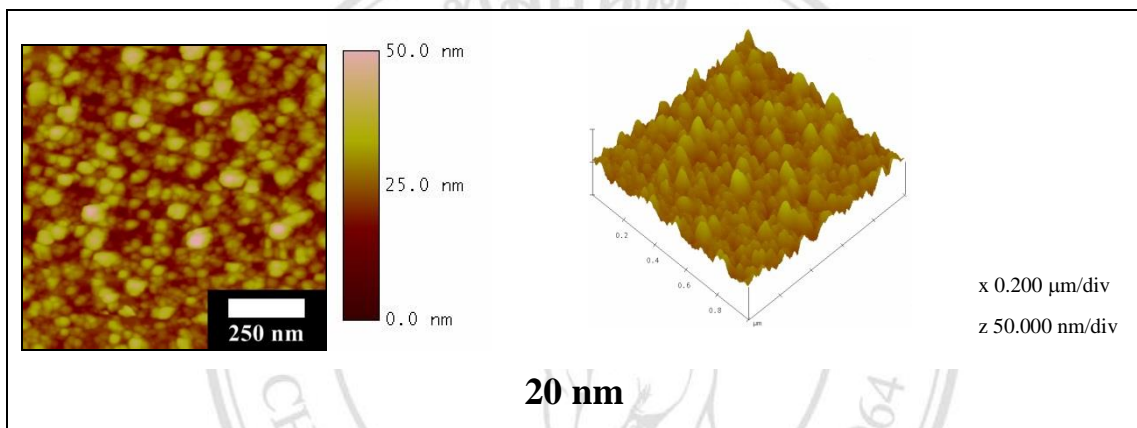
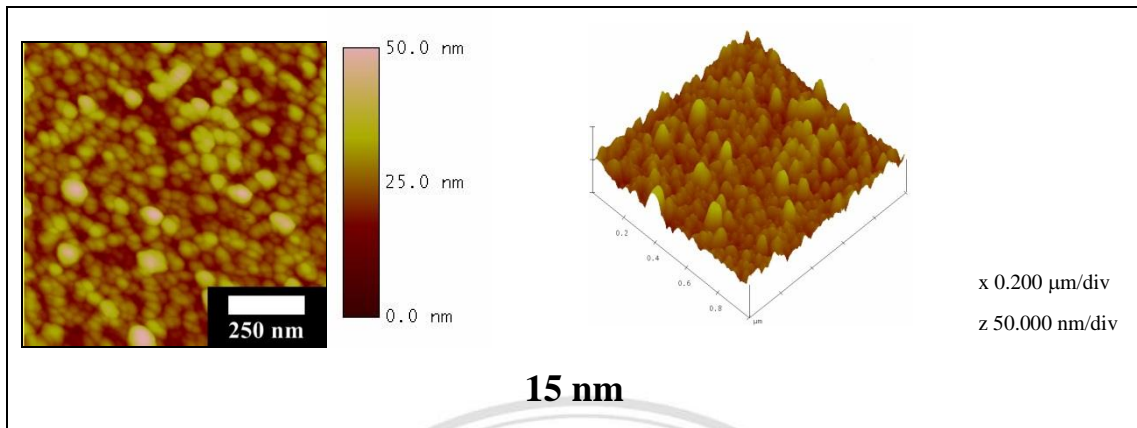


Figure 5.6 AFM images of ITO/Au/ITO multilayer films with different Au intermediate layer thicknesses (continued).

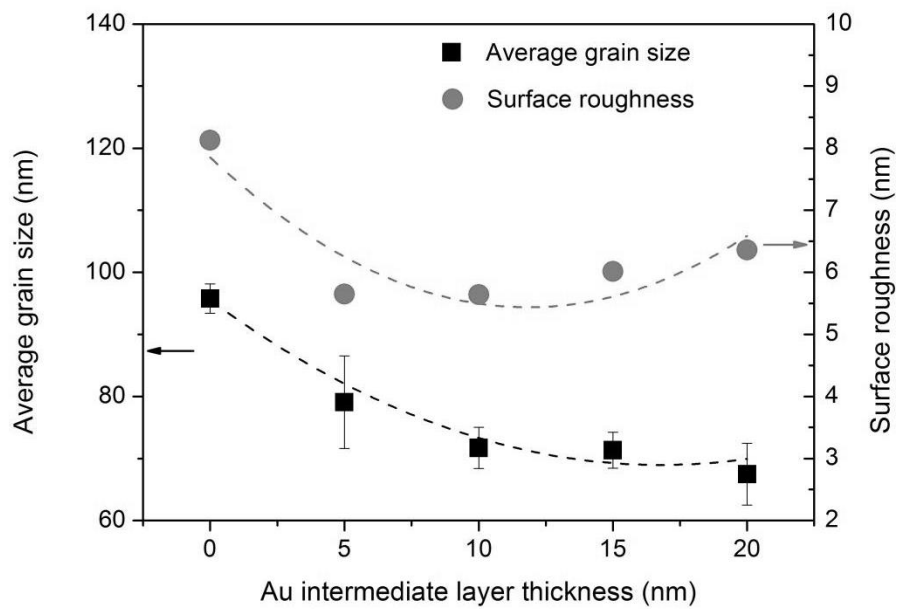


Figure 5.7 Average grain size and surface roughness of ITO/Au/ITO multilayer films with different Au intermediate layer thicknesses.

The average grain size and surface roughness of films were obtained from the SEM and AFM images, respectively. The trends of these values are shown in Fig. 5.7. It was found that the average grain size of the single layer was the maximum at 95.79 nm and decreased slightly with increasing Au intermediate layer thickness. The surface roughness of multilayer films reduced with the Au intermediate layer. *Gritan et al.* [81] reported that the thin metallic layer does not influence the morphology of the next oxide layer as the bottom oxide layer controls the morphology of the top oxide layer. The result of this previous research was opposite to my research. It was found that the low Au intermediate layer thickness film (5 nm) exhibited cubical shape same as the morphology of ITO single layer. Then the morphology of the multilayer films changed to a spherical shape with increasing Au layer thickness higher than 5 nm. This shape was similar to the grain shape of the Au layer. It was proposed that the grain shape of Au layer controlled the grain shape of the top ITO layer. The morphologies of Au layers with different thickness coated on ITO single layer films are shown in Figure 5.8. It was found that the grain size of Au (~ 23 nm) was smaller than for ITO and the surface roughness of the Au layer decreased with increasing Au layer thickness (Figure 5.9). Moreover, the Au intermediate layer thickness effectively promoted crystallization in the (222) plane of the top ITO layer due to this layers growth in the same direction as the Au layer. Hence, the Au intermediate layer thickness effect on the grain direction, grain size and grain shape of top ITO layer.

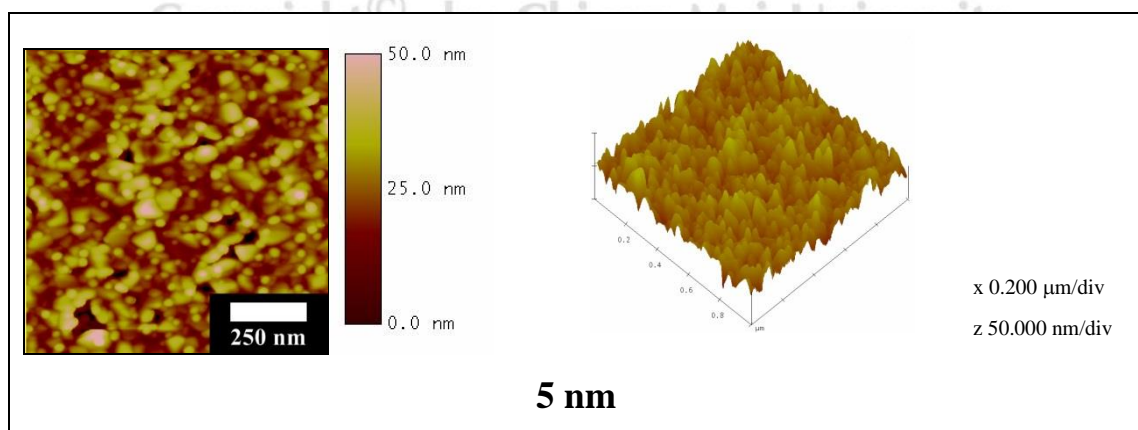


Figure 5.8 AFM images of Au layer with different Au layer thicknesses.

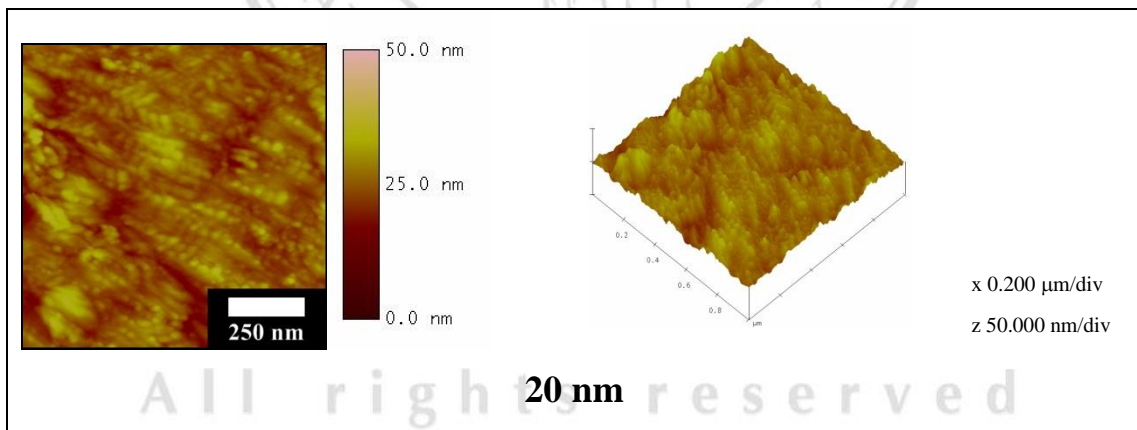
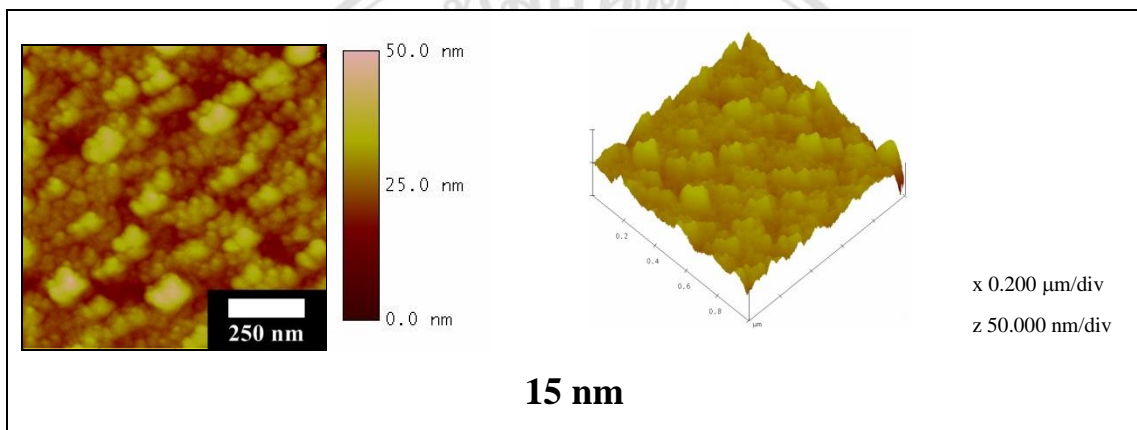
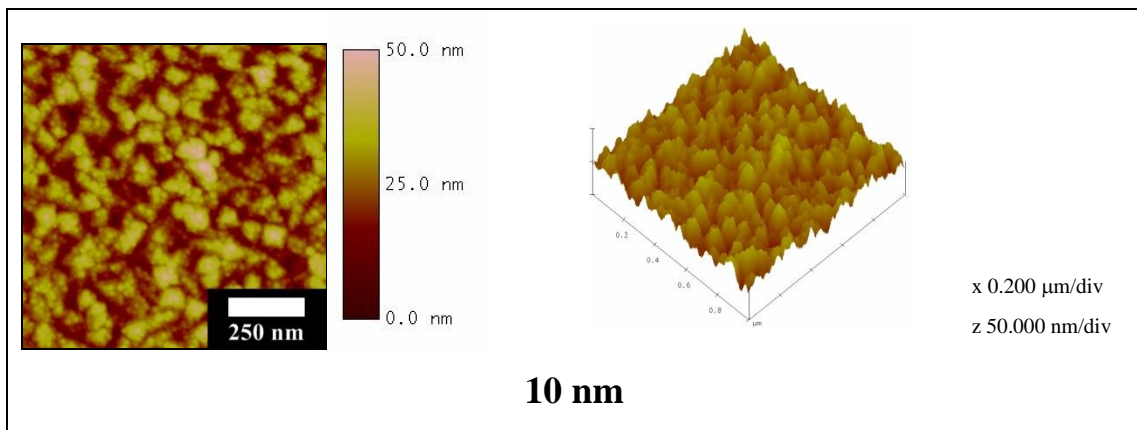


Figure 5.8 AFM images of Au layer with different Au layer thicknesses (continued).

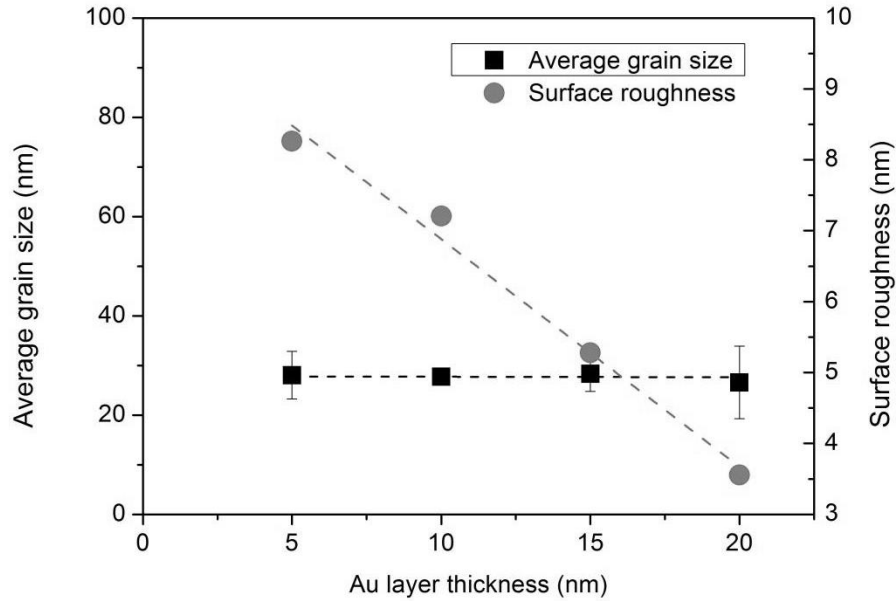
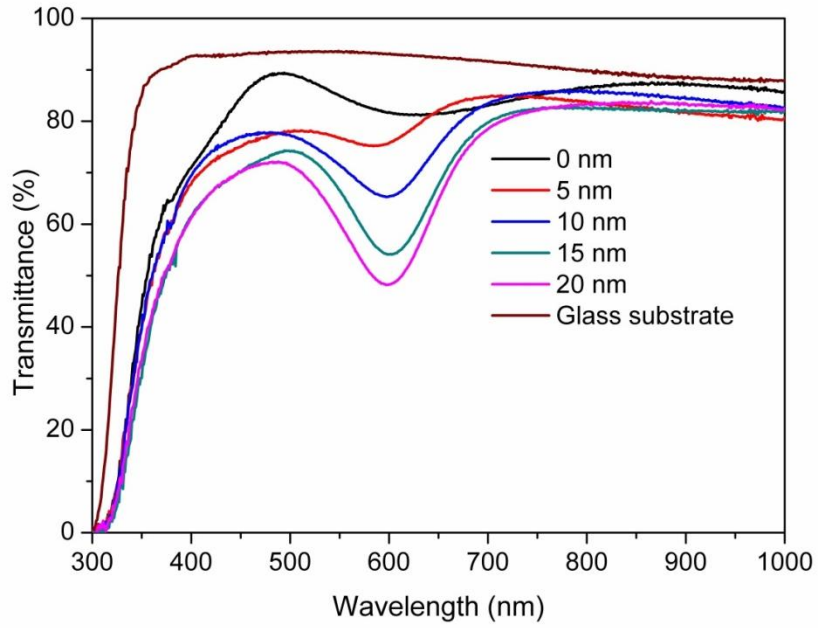


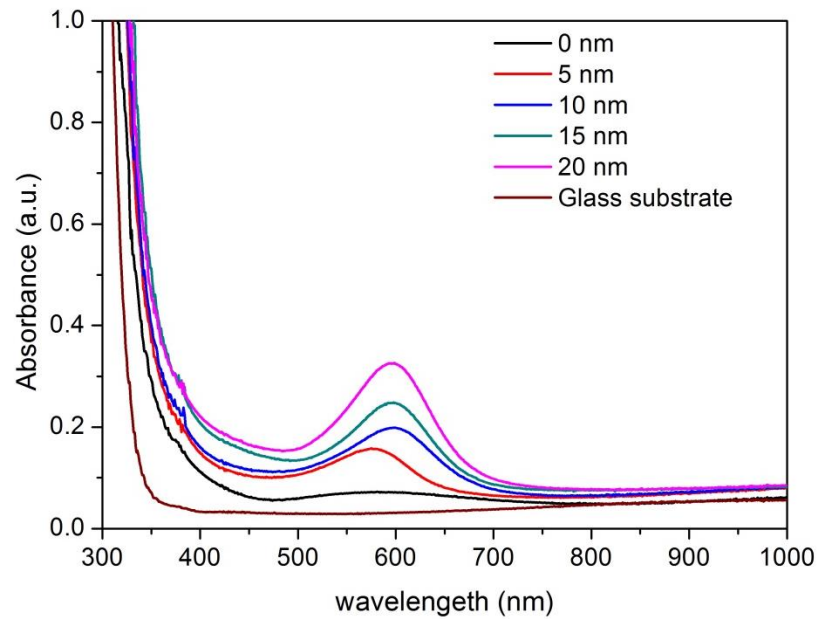
Figure 5.9 Average grain sizes and surface roughness of Au layer with different Au layer thicknesses.

5.2.4 Optical properties

The transmittance and absorbance spectra over the wavelength range 300-1000 nm of the glass substrate and ITO/Au/ITO multilayer films with different Au intermediate layer thickness are shown in Figure 5.10. It was found that the transmittance of films decreased with increasing Au intermediate layer thickness. This behavior of films occurred from the addition of the metallic layer in the multilayer films, as the layer reduced the transmittance in the multilayer films [8, 53, 82]. Moreover, the multilayer films had an extra absorption peak near 600 nm caused by absorbance of the Au layer [83].



(a) Transmittance

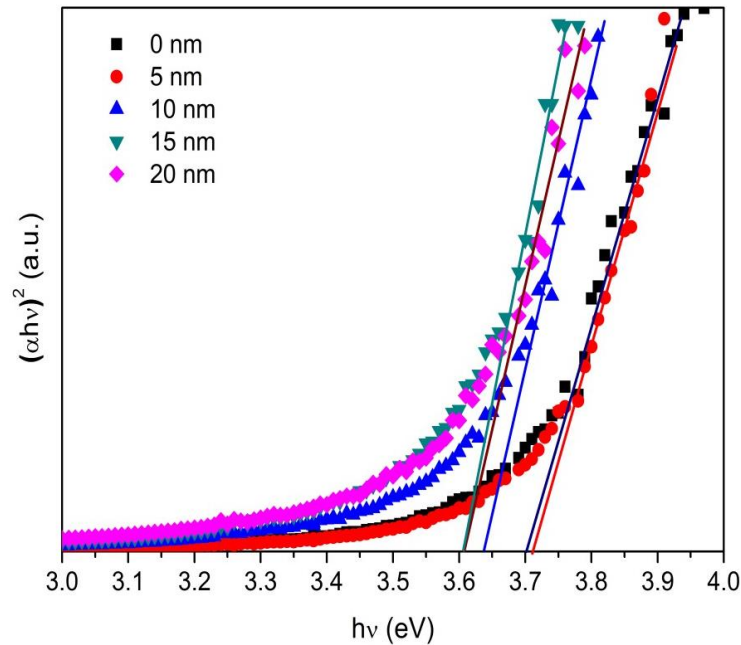


(b) Absorbance

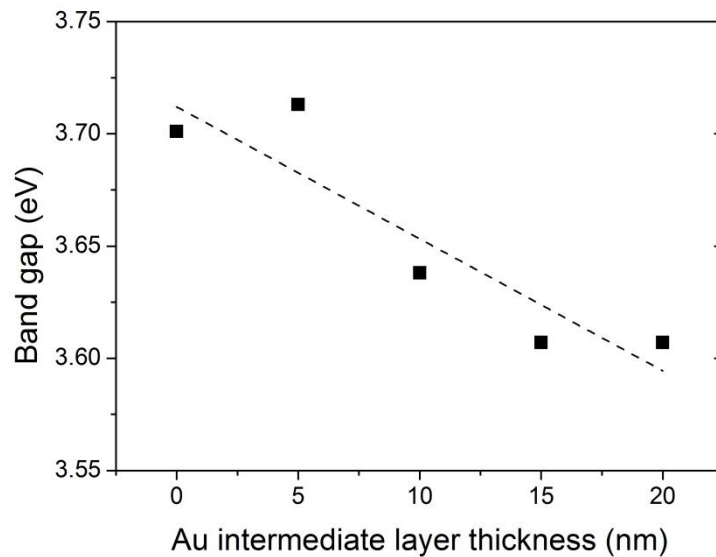
Figure 5.10 Transmittance (a) and absorbance (b) spectra of ITO/Au/ITO multilayer films with different Au intermediate layer thicknesses.

The band gap was evaluated from the transmittance spectra by using Tuac's relationship in equation 3.8. The $(\alpha h\nu)^2$ versus $h\nu$ plots of all films are shown in Figure 5.11 (a) and the intercept of $(\alpha h\nu)^2$ on the x -axis of these

plots gave the value of the direct band gap. The trend of band gap values of multilayer films is shown in Figure 5.11 (b). It was found that the trend of the band gap of films decreased with increasing Au intermediate layer thickness. This behavior occurred due to many interaction effects of free carriers [66,79] of the Au intermediated layer.



(a) $(\alpha h\nu)^2$ versus $h\nu$ plots



(b) Band gap

Figure 5.11 The $(\alpha h\nu)^2$ versus $h\nu$ plots (a) and the band gap of ITO/Au/ITO multilayer films with different Au intermediate layer thicknesses.

5.2.5 Electrical properties

The sheet resistance and the resistivity of ITO/Au/ITO multilayer films with different Au interlayer thickness are shown in Figure 5.12. The resistivity was calculated from resistance and thickness (Table 5.1) by equation 3.10. It was found that the ITO single layer film showed highest sheet resistance and resistivity of 1416 Ω/sq and $3.41 \times 10^{-2} \Omega\cdot\text{cm}$, respectively. The resistivity of multilayer films decreased with increasing Au intermediate layer thickness. This behavior could be explained as due to a lot of free electrons in the Au layer, which increased the carrier concentration in the multilayer films and improved the conductivity of the films [66,79]. This behavior was observed in other work [54,84].

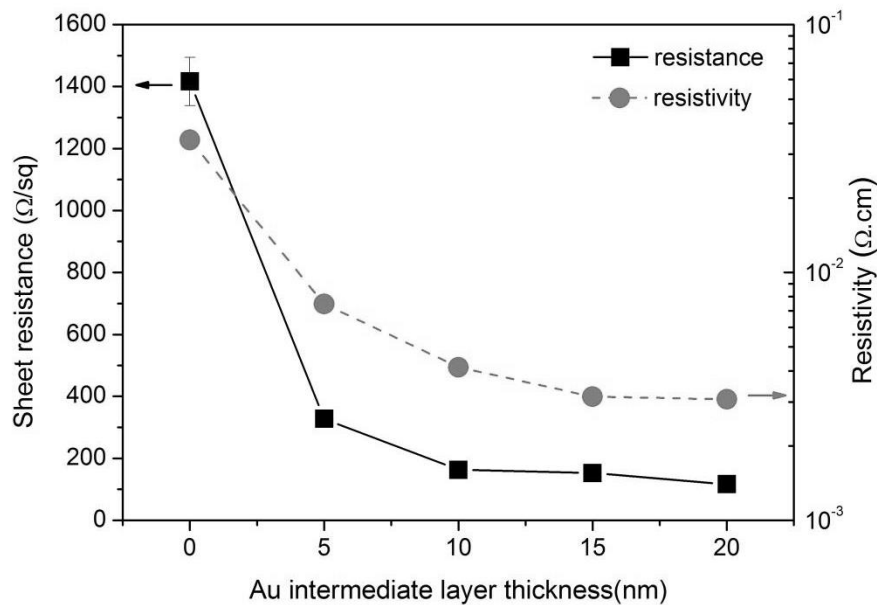


Figure 5.12 The sheet resistance and the resistivity of ITO/Au/ITO multilayer films with difference Au intermediate layer thicknesses.

The total resistance of the multilayer was a combination of the resistance of the three layers in equation 5.1 [82,84]:

$$1/R_{\text{Total}} = 1/R_{\text{Au}} + 2/R_{\text{ITO}} \quad (5.1)$$

Au metal has a low electrical resistivity value of $2.4 \mu\Omega\cdot\text{cm}$ [8]. After the addition of an Au layer in an ITO film, the total resistivity of the multilayer film should be lower than for an ITO single layer film. Hence, ITO/Au/ITO

multilayer films have enhanced electrical properties, with lower resistivity than ITO single layer films of the same thickness.

5.2.6 Performance

Although the Au layer improved the conductivity of films, this layer reduced the transmittance of the films too. Therefore, the best condition of this work cannot be expected from the lowest resistivity conditions. The performance of film was used to indicate the best condition of films in this section, which is predicting the transparent conducting film properties of a material from its fundamental electrical and optical constants. The performance of a film was evaluated by the figure of merit (Φ_{TC}), which was derived to predict the transparent electrode properties of a material from its fundamental electrical and optical constants. Φ_{TC} is defined by G. Haacke [85] as:

$$\Phi_{TC} = T^{10}/R_s \quad (5.2)$$

where T is the transmission coefficient at 550 nm (fraction of 1) of these multilayer films, which are listed in Table 5.3 and R_s is the sheet resistance (Figure 5.12) of the multilayer films. Φ_{TC} is shown in Figure 5.13 and reaches a highest value of $2.30 \times 10^{-4} \Omega^{-1}$ for the ITO/Au/ITO multilayer film with a 10 nm Au intermediate layer. Therefore, the film with 10 nm Au interlayer has the best performance of these samples.

Table 5.3 The transmission coefficient at wavelength of 550 nm of ITO/Au/ITO multilayer films with difference Au intermediate layer thicknesses.

Au intermediate layer thickness (nm)	Transmittance coefficient at 550 nm
0	0.85
5	0.77
10	0.72
15	0.67
20	0.60

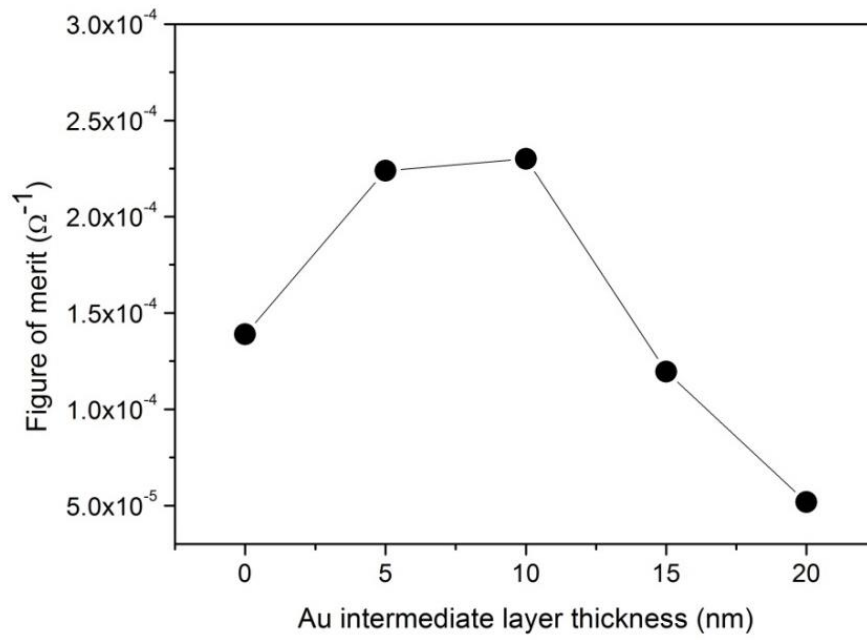


Figure 5.13 The figure of merit of ITO/Au/ITO multilayer films with different Au intermediate layer thicknesses.

ลิขสิทธิ์มหาวิทยาลัยเชียงใหม่
Copyright© by Chiang Mai University
All rights reserved